

Modeling the analog control of a DC machine in a MATLAB environment: Case of a shunt machine

Bokovi Yao¹, Akoro Edjadessamam², and Tevi Kokou Sévérin³

¹CERME (Centre d'Excellence Régional pour la Maîtrise de l'Electricité, Laboratory of Research in Engineering Sciences (LARSI), Université de Lomé, Lomé, Togo

²CERME (Centre d'Excellence Régional pour la Maîtrise de l'Electricité, Laboratory of Research in Engineering Sciences (LARSI), Université de Lomé, Lomé, Togo

³EPL (Ecole Polytechnique de Lomé), Université de Lomé, Lomé, Togo

Copyright © 2024 ISSR Journals. This is an open access article distributed under the *Creative Commons Attribution License*, which permits unrestricted use, distribution, and reproduction in any medium, provided the original work is properly cited.

ABSTRACT: This paper studies the control of a DC machine in a Matlab/Simulink environment, more specifically the shunt machine. We first highlight the modeling of a shunt machine and then control it by acting on each parameter, first in open loop, then in closed loop, while studying the system's performance. Finally, introduce the appropriate correction to improve system performance. The second part consisted in simulating the operation of the shunt-excited DC machine in a Matlab/Simulink environment. The more the electric motors are loaded, the lower the rotational speed. In order to bring the motor speed back to its nominal value, two types of control were proposed in this work: control by variation of the armature voltage U_a and control by variation of the excitation current I_e . Simulation of these two types of control, in our case using Matlab/Simulink software, showed the strengths and weaknesses of each type of control, depending on whether a PI corrector is integrated or not.

KEYWORDS: Closed loop, Open loop, Closed loop transfer function, Open loop transfer function, DC machine, Proportional-Integral-Derivative.

1 INTRODUCTION

DC machines have a wide range of applications. Depending on their power, we distinguish: low-power machines (a few W) used in servomechanisms (washing machine programmers, dishwashers, etc.); motors for tool machines or lifting gear (1 to 300 kW) [1], [2]; high-power motors (up to 10 MW) equipping certain locomotives; universal motors that can operate in both DC and AC (series motor for small household appliances: vacuum cleaner, centrifuge, etc.). DC machines are practically no longer used for power generation. They have been replaced by alternators combined with rectifiers. However, the reversibility of DC motors enables them to operate transiently as generators during the braking phases of tool machine, hoist and traction motors. [2] The generator operation of a DC machine is used to measure angular speeds (tachometer). DC motors have a high starting current, which can lead to their destruction. In addition, the speed and torque of the motor vary in steady-state operation, leading to problems of stability and accuracy. At high loads, the motor comes to a standstill, and the current reaches a maximum, leading to the risk of destruction through overheating [3]. Existing solutions to limit the armature current at start-up are the use of starting rheostats and starting at a reduced supply voltage [3].

In order to solve this problem, it is necessary to propose a servo-control with a suitable corrector for greater precision. Modeling the control of DC machines will enable us to study the speed variation problems encountered on these machines and to provide appropriate solutions. It is within this framework that this paper deals with DC machine control modeling in a Matlab environment. The main objective, in a Matlab environment, is to define and model the control of a DC machine first by a

continuous speed control system ω_m , and then to implement this control in order to control the variable speed drive of said machine. The paper is organized as follow: In Section 2, state of the art is presented. Section 3 deals with the methods and materiel. Section 4 presents the methodology. Section 5 presents the results analysis and Section 6 concludes the paper.

2 STATE OF THE ART

DC machines are electromechanical energy converters, i.e., they are rotating machines that transform electrical energy into mechanical energy (motor); mechanical energy into electrical energy (generator). DC machines have two operating modes: generator operation and motor operation.

2.1 GENERATOR OPERATION

Fig. 1 shows a permanent magnet DC machine.

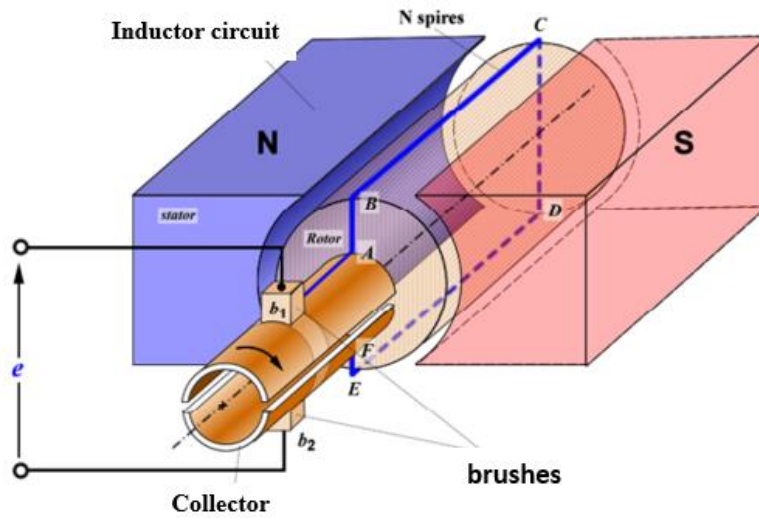


Fig. 1. Switching principle of a DC machine

The winding (ABCDEF) rotates between the N and S poles of a magnet (in conventional machines, the N and S poles are due to inductive circuits). The rotor attached to the spiral is driven by an external device (motor, wind, etc.). The rotational motion of the rotor is given by equation (1):

$$\theta = \omega t + \theta_0 \tag{1}$$

θ_0 being the initial position of the rotor with respect to the reference axis. The variation of the magnetic field in the air gap is given by equation (2):

$$B(\theta) = B_M \cos(\theta) \tag{2}$$

Fig. 2 shows the variation of the magnetic field in the air gap as a function of angular position [4].

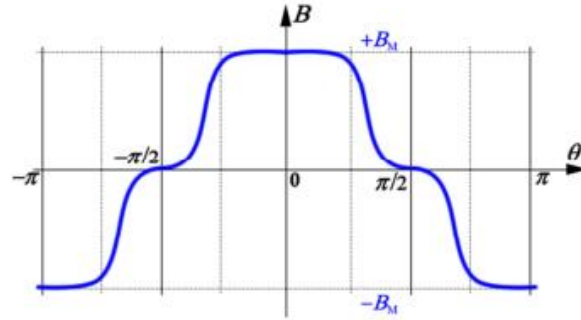


Fig. 2. Magnetic field variations in the air gap as a function of angular position

2.2 MOTOR OPERATION

as shown in Fig. 3, Since the DC machine is reversible, if a DC current flows through the coil (ABCDEF) placed in a magnetic field due to the magnets, Laplace’s law states that, in the presence of the commutator, it will be subjected to a torque which drives the rotor in rotation and whose intensity is defined by relationship (3):

$$C_e = f_r R = F \cdot OH = BILR \cos(\omega t + \theta_0) \tag{3}$$

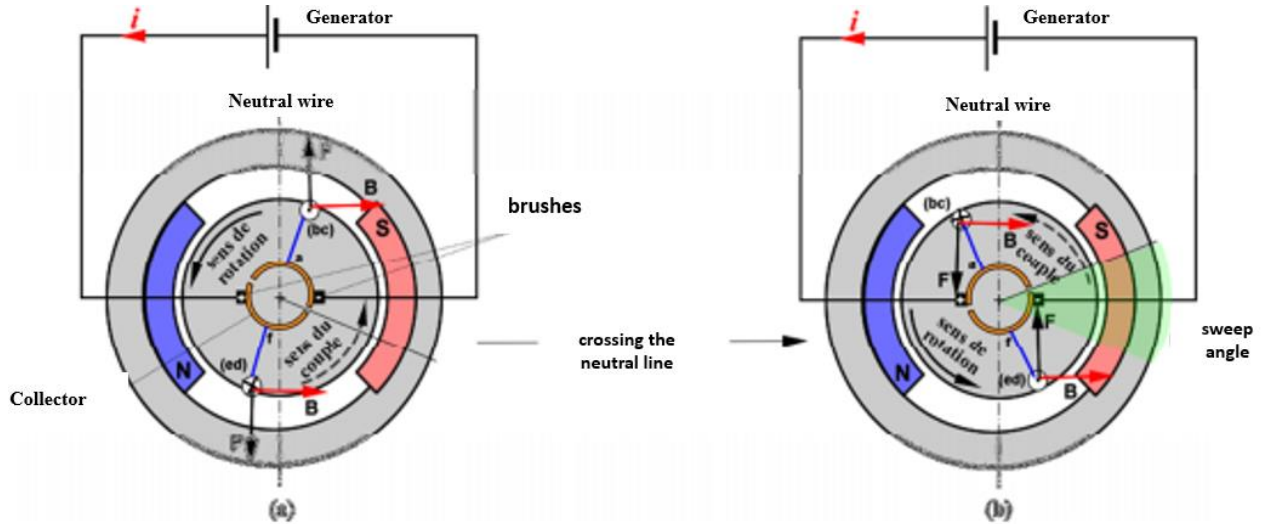


Fig. 3. Collector/brush assembly operation

Fig. 3 shows the pattern of torque vibrations as a function of time.

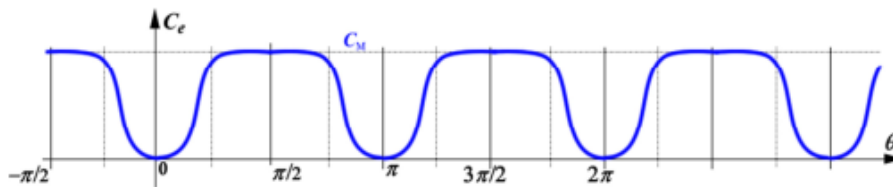


Fig. 4. Torque vibrations as a function of time

In a real machine, several conductors are distributed along the air gap, and the machine is multipolar. It is clear that the torque curve will be the same as that of the F.E.M in generator operation, so that we obtain a practically rectified torque. Fig. 5 shows the torque curve for a motor with two conductors offset by 90 degrees.

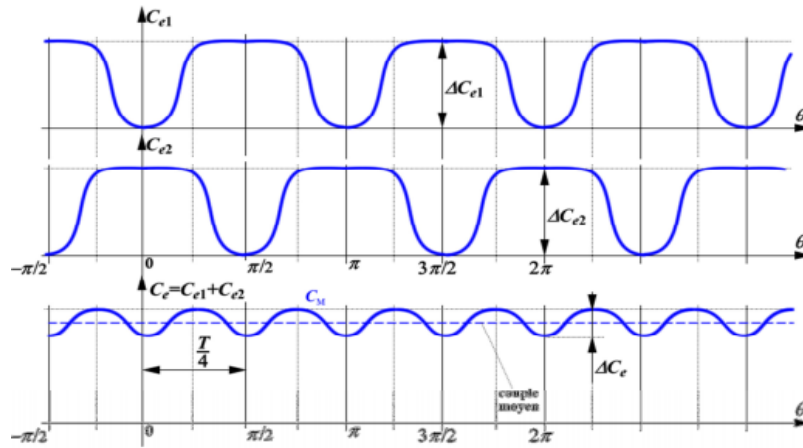


Fig. 5. Reduced torque ripple

3 METHODS AND MATERIALS

3.1 METHODS

To study the operation of the motor, each component must be modeled as an electrical component. The stator is modeled as a resistance R_e in series with an inductance L_e , while the rotor is modeled as a resistance R_a in series with an inductance L_a , both in series with a back electromotive force E . The motor's supply voltage is U_a . By applying the Laplace transform to the electrical equations of the rotor and the electromechanical equations, the block diagram of the DC motor is obtained.

3.2 MATERIALS

SIMULINK, a MATLAB software for modelling and simulation, is our tool for implementing and simulating the shunt-excited DC motor model.

4 METHODS AND MATERIALS

Fig. 6 illustrates the different stages of the control system for the shunt-excited DC motor.

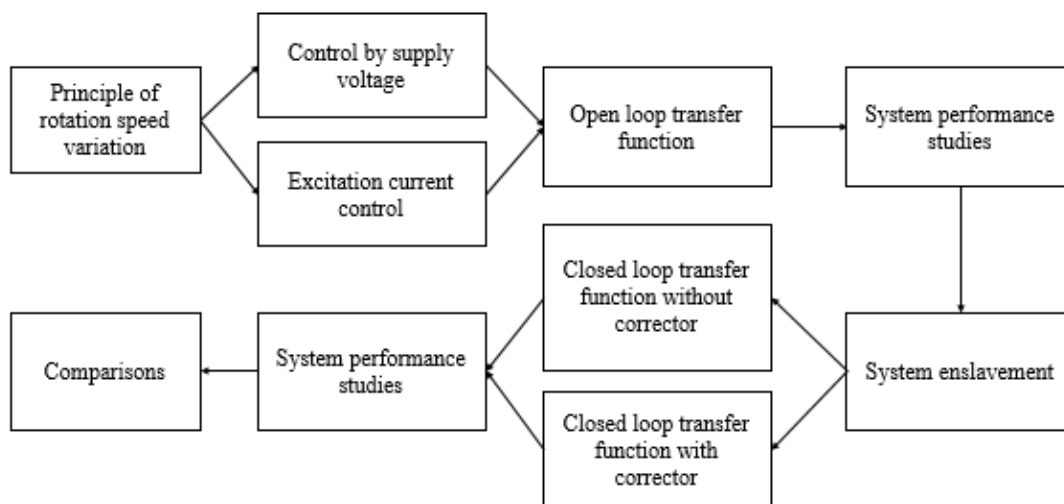


Fig. 6. The different stages of the speed control of the direct current motor with shunt excitation

4.1 PRINCIPLE OF SPEED VARIATION FOR A SHUNT-EXCITED DC MOTOR

To study the operation of the motor, each component needs to be modeled as an electrical component. Fig. 7 presents the electrical model of the shunt-excited DC motor [5].

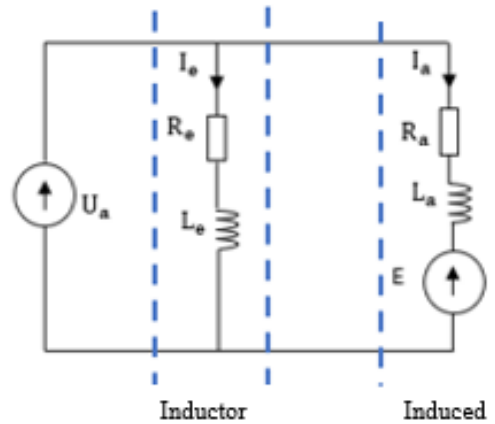


Fig. 7. Electrical model of the DC motor with shunt excitation

Electrical equation of the armature:

$$u_a(t) = e(t) + R_a i_a(t) + L_a \frac{di_a(t)}{dt} \tag{3}$$

The electrical equation of the field winding is:

$$u_a(t) = R_e i_e(t) + L_e \frac{di_e(t)}{dt} \tag{4}$$

Electromechanical Equation:

$$E(t) = k_e \Phi(I_e) \omega_m(t) \tag{5}$$

$$\Phi(I_e) = L_{ea} I_e(t) \tag{6}$$

$$C_e(t) = k_c \Phi(I_e) I_a(t) \tag{7}$$

Mechanical equation:

$$c_e(t) - c_r(t) = B \omega_m(t) + J \frac{d\omega_m(t)}{dt} \tag{8}$$

In steady state $\frac{di_a(t)}{dt} = 0$, and by substituting the back electromotive force (EMF) with its value into equation (5), we obtain:

$$\omega_m = \frac{U_a - R_a I_a}{k_e \Phi(I_e)} \tag{9}$$

According to equation (9), speed variation is possible by adjusting the following parameters:

- U_a : the supply voltage
- I_e : the excitation current

In this work, we will study the variation in the speed of the DC motor by changing the supply voltage.

4.2 MODELLING OF THE SHUNT-EXCITED DC MOTOR

By applying the Laplace transform to equations (3) and (8), we obtain equations (10), (11), and (12):

$$\frac{I_a(P)}{U_a(P) - K\omega_m(P)} = \frac{1}{R_a + L_a P} \tag{10}$$

$$C_e(P) = K I_a(P) \tag{11}$$

$$\frac{\omega_m(P)}{C_e(P) - C_r(P)} = \frac{1}{B + J P} \tag{12}$$

From equations (10), (11), and (12), we obtain the block diagram of the shunt-excited DC motor, as presented in Fig.8.

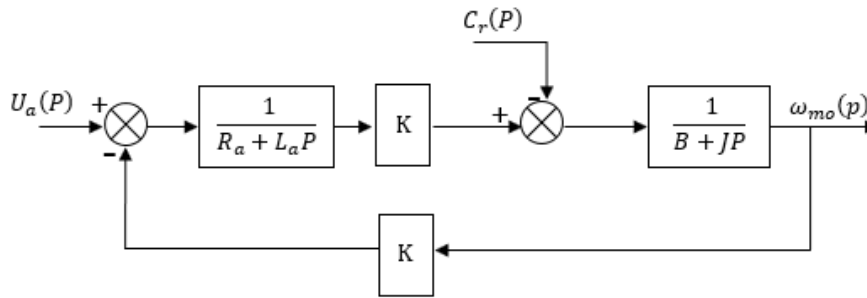


Fig. 8. Block diagram of MCC with shunt excitation

4.3 IMPLEMENTATION OF THE SHUNT-WOUND DC MOTOR MODEL IN MATLAB

Fig. 9 shows the model of the shunt-wound DC motor implemented in MATLAB/Simulink.

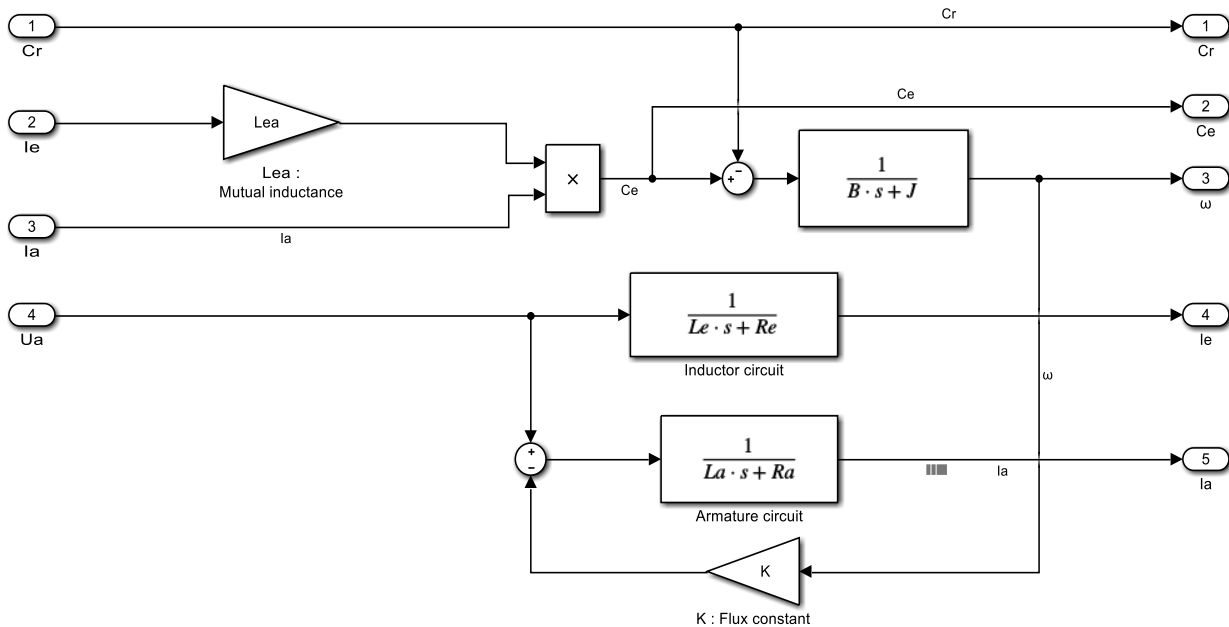


Fig. 9. Block diagram of MCC with shunt excitation under Simulink

5 RESULTS AND DISCUSSION

This section presents the modeling of a shunt-excited DC motor in a MATLAB/Simulink environment and the simulation results of the system both without a controller and with a PI controller.

The motor parameters are presented in Table 1.

Table 1. Shunt excitation current motor parameters

U_a	I_a	I_e	R_a	R_e	L_a	L_e	L_{ea}	ω_m	J_m	B_m	K	C_n	P
220 V	16 A	1,32 A	1,35 Ω	65,15 Ω	0,0059 H	8,35 H	1,07 H	1500 trs/min	0,036 kg.m ²	0,0045 Nm/rad/s	1,41 V/rad/s	19 N.m	3 kW

5.1 OPEN-LOOP OPERATION

In this section, we will perform an open-loop simulation of the shunt-excited DC motor. Fig. 10 illustrates the block diagram of the shunt-excited DC motor in open-loop configuration.

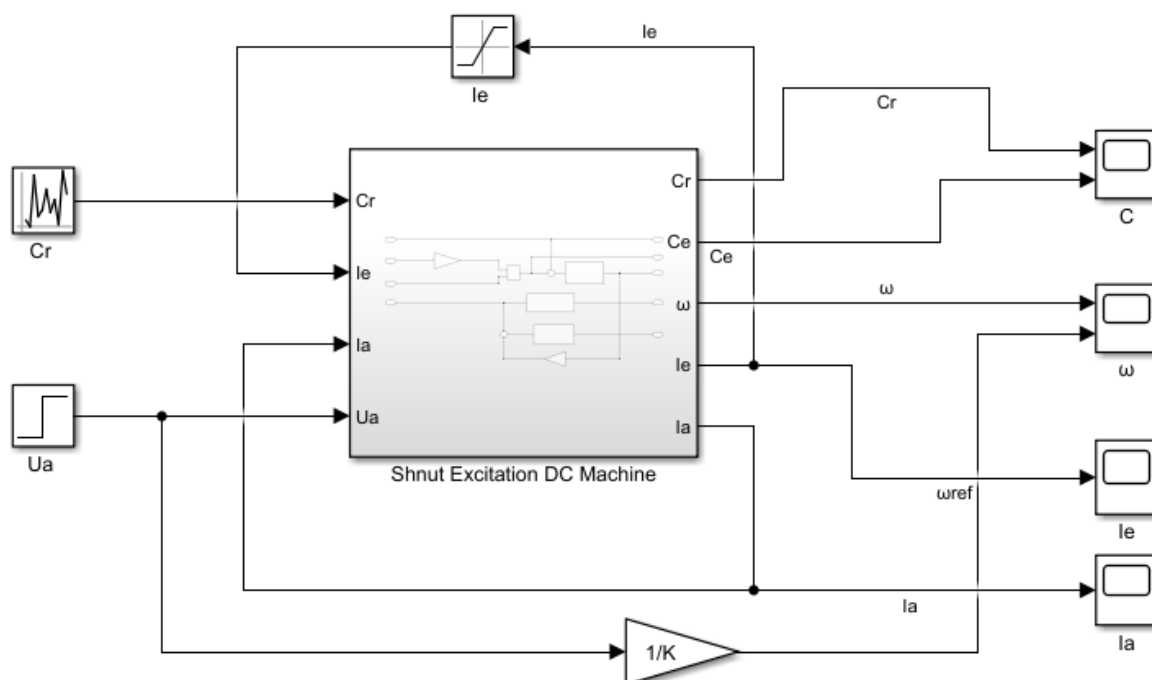


Fig. 10. Block diagram of the direct current machine with open loop shunt excitation

The simulation results show the behavior presented in Fig. 11, which depicts the rotational speed of the shunt-excited DC motor as a function of time in open-loop operation, controlled by the supply voltage and subjected to a variable load ranging from 0 to C_n during the simulation period.

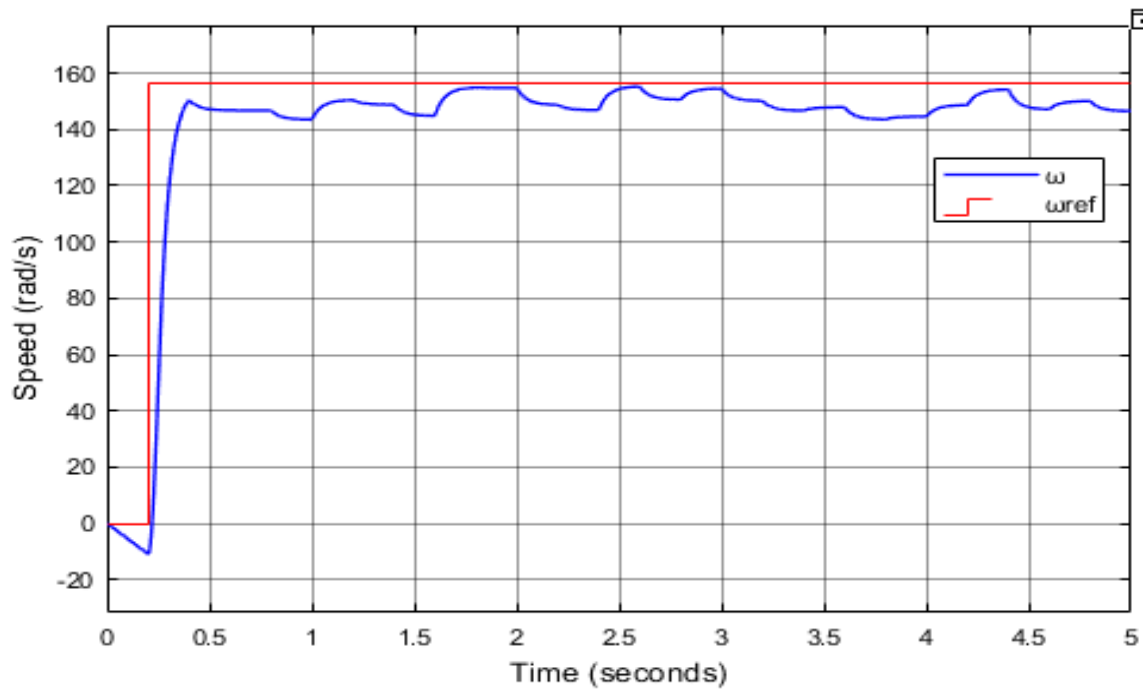


Fig. 11. Change in speed of the shunt excitation direct current machine subjected to a variable load in open loop

Fig.12 shows the variation of the armature current of the shunt-excited DC motor under supply voltage control and subjected to a variable load during the simulation period.

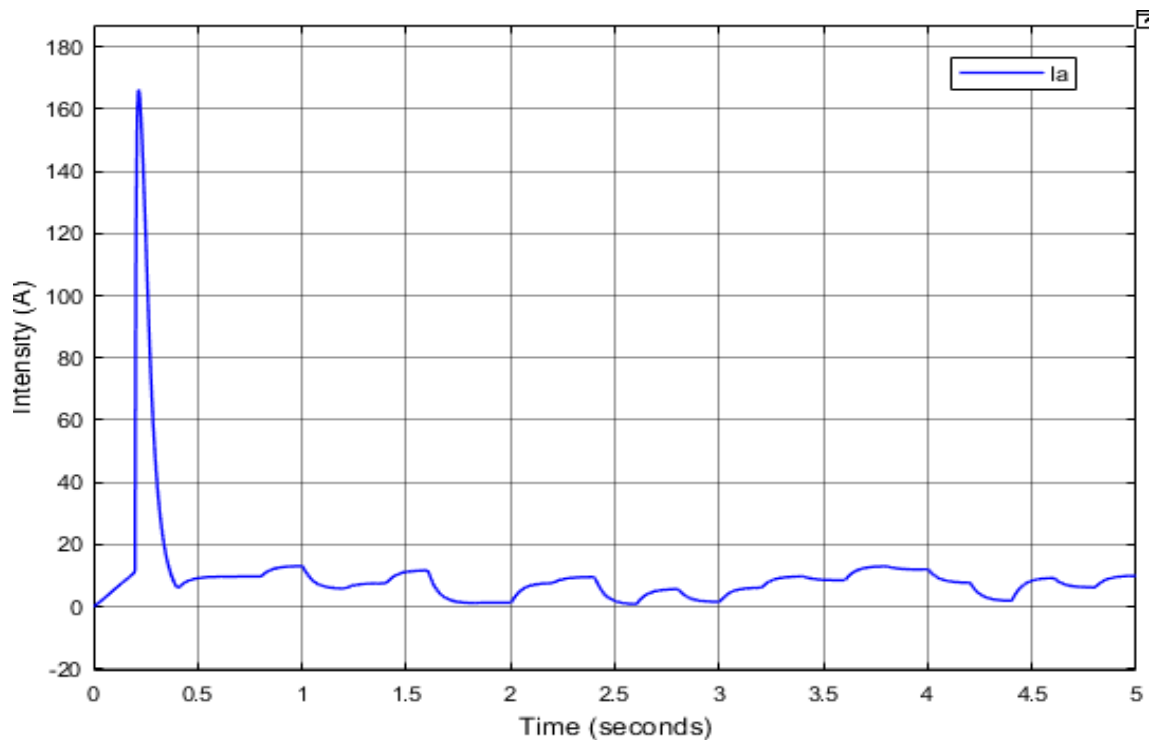


Fig. 12. Evolution of the armature current of the direct current machine with shunt excitation subjected to a variable load in open loop

Considering these results (Fig. 11 and Fig. 12), we observe that changes in load lead to variations in the rotational speed and armature current of the shunt-excited DC motor. An increase in load results in a higher armature current and a larger steady-state error. Consequently, the system's precision decreases [6], [7].

5.2 CLOSED-LOOP OPERATION WITHOUT CONTROLLER

In this subsection, we analyze the performance of the shunt-excited DC motor in a closed-loop configuration without any additional control elements.

Fig. 13 shows the block diagram of the DC motor in closed-loop operation with a variable load and an amplification gain K_A . With a supply voltage of 220V, the oscilloscopes allow visualization of the load torque, motor torque, reference signal, rotational speed, excitation current, and armature current.

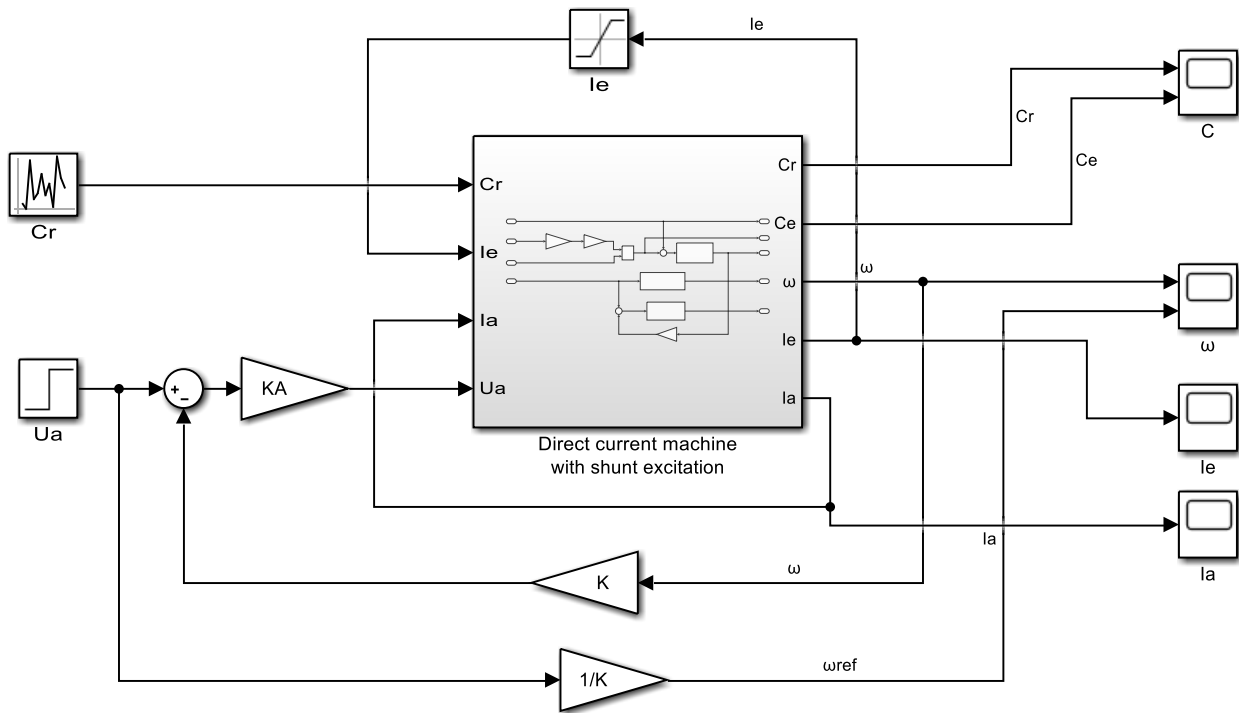


Fig. 13. Block diagram of the direct current machine with closed loop shunt excitation without a corrector

The simulation results will be presented in Fig. 14 and Fig. 15, with the simulation time set to 2 seconds. Fig. 14 illustrates the variation in the speed of the shunt-excited DC motor in closed-loop operation with supply voltage control as a function of time for different values of K_A , subjected to a variable load. Fig. 15 shows the variation in the armature current of the DC motor in closed-loop operation with supply voltage control, subjected to a variable load, for several values of the amplification gain K_A .

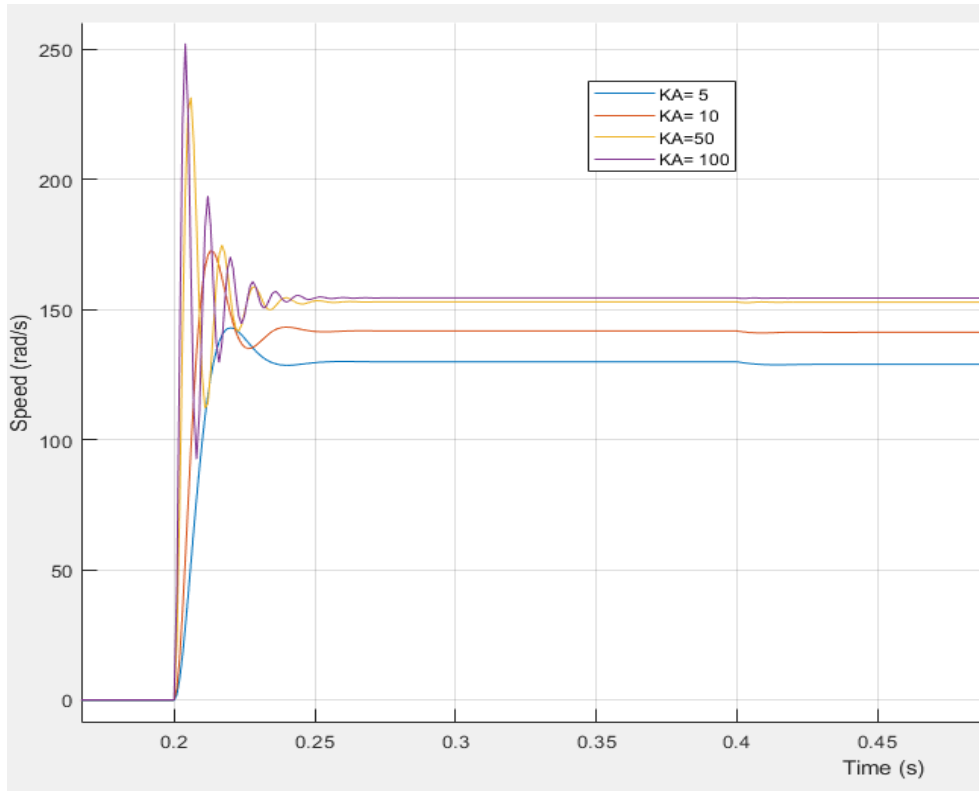


Fig. 14. Evolution of the speed of the direct current machine with closed-loop shunt excitation without a corrector as a function of the amplification gain K_a

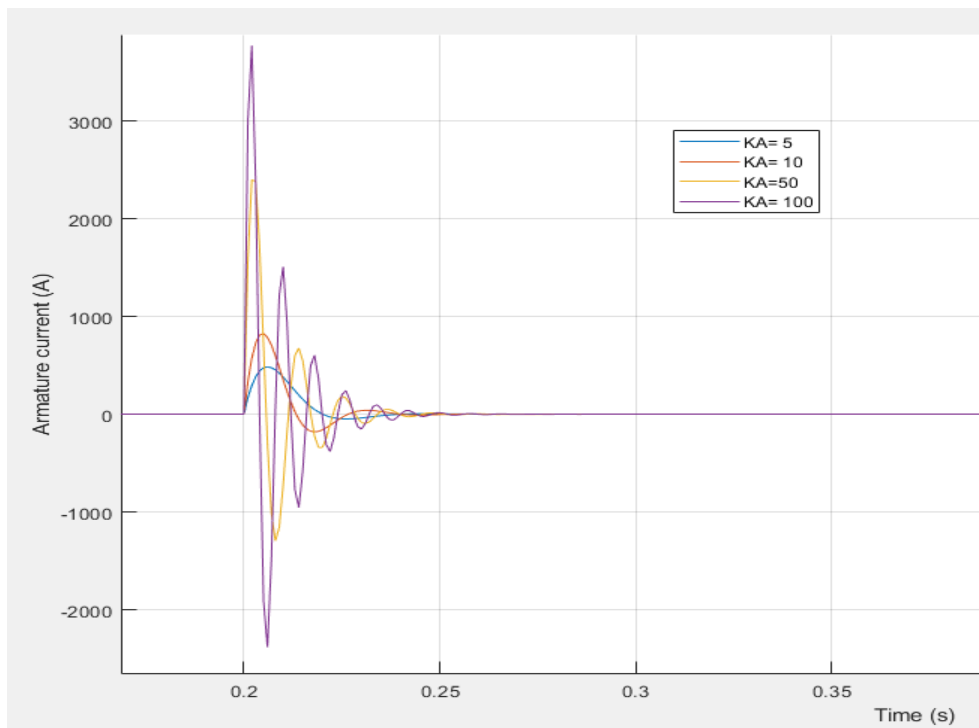


Fig. 15. Induced current of the direct current machine with closed loop shunt excitation without a corrector as a function of the amplification gain K_a

Table 2 presents the system’s steady-state performance in closed-loop operation without a controller, controlled by supply voltage and subjected to a variable load, for different values of the amplification gain K_A .

Table 2. Steady state performance of the closed loop direct current machine in control by supply voltage without a corrector subjected to a variable load for different values of the amplification gain K_A

Performances	$K_A = 5$	$K_A = 10$	$K_A = 50$	$K_A = 100$
$\omega_{BF\ SC\ max}$ (rad/s)	142.99	172.67	231.54	252.31
$\omega_{BF\ SC\ moyen}$ (rad/s)	128.97	141.26	152.84	154.42
$\varepsilon_{BF\ SC\ moyen}$ (rad/s)	28.03	15.74	4.16	2.58
RMSE	28.03	15.69	4.14	2.56
Coef corr :R	-0.6204	-0.5078	-0.4935	-05096
$\tau_{m\ BF\ SC}$ (ms)	10	7.5	3.5	2.5
$\tau_r\ BF\ SC$ (ms)	-	10.5	10.5	10.00
$I_{a\ BF\ SC\ max}$ (kA)	0.48	0.82	2.3	3.8
$I_{a\ BF\ SC\ moyen}$ (A)	6.63	6.66	6.69	6.69
Pole(Hz)	-100	-133,33	-285,71	-400
Stability	Stable	Stable	Stable	Stable

It is observed that the discrepancy between the setpoint and the steady-state rotational speed has decreased. For large values of K_A , the discrepancy tends towards zero. Increasing the amplification gain leads to a reduction in the steady-state error. Increasing the amplification gain also leads to a decrease in the rise time in closed-loop without a compensator. The system becomes faster as the amplification gain increases. A peak in the armature current is observed at startup. This peak in armature current has the same variation direction as the amplification gain. As the amplification gain increases, the startup current also increases [8].

6 CONCEPT OF CLOSED-LOOP CONTROL WITH A PI CONTROLLER

Fig. 16 presents the block diagram of the DC motor in a closed-loop system with voltage control using a PI controller, subjected to a variable load ranging from 0 to C_n [9], [10].

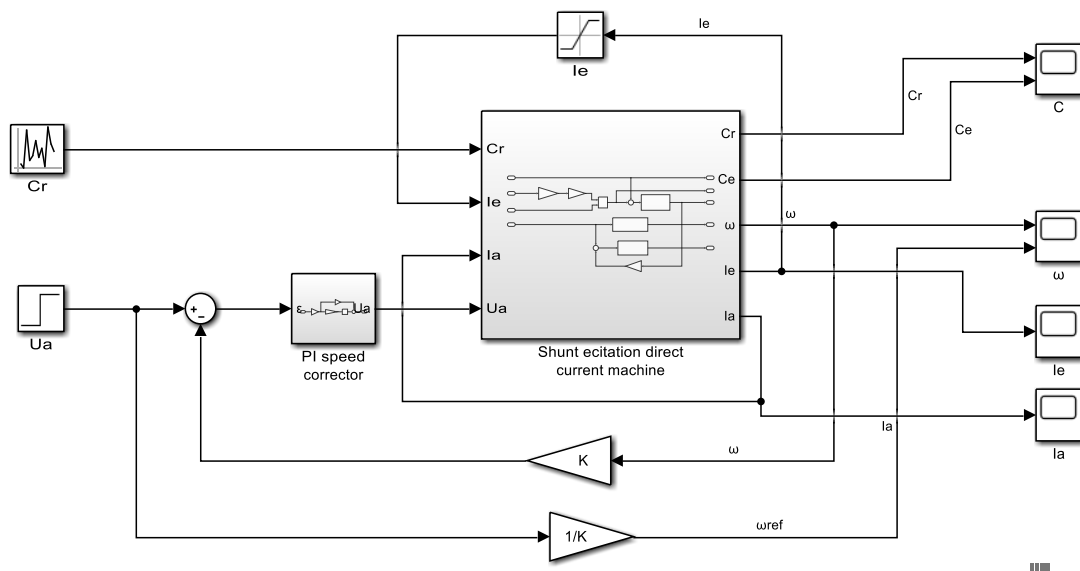


Fig. 16. Block diagram of the direct current machine with closed loop shunt excitation with PI corrector

The simulation results are presented in Fig. 17 and Fig. 18, with the simulation time set to 2 seconds. Fig.17 shows the variation in the motor speed in the frequency domain with a PI speed controller operating with different values of the amplification gain KA applied to the power supply voltage.

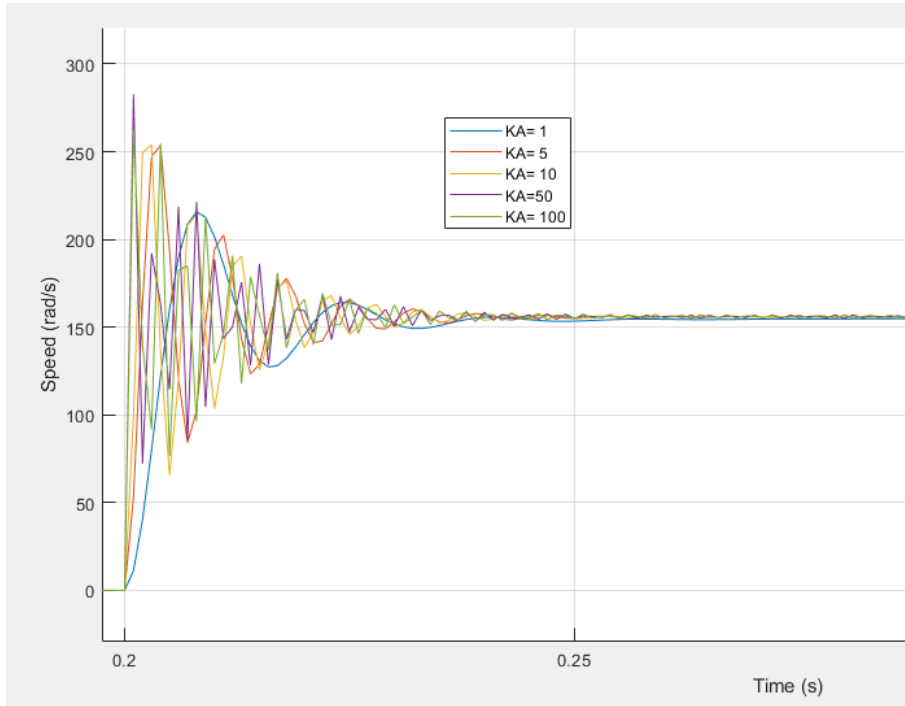


Fig. 17. Evolution of the speed of the closed loop shunt excitation current machine with a PI corrector

Fig.18 presents the variation in the armature current of a shunt-wound DC motor over time in a closed-loop system with a PI controller, using power supply voltage control for different values of the amplification gain KA.

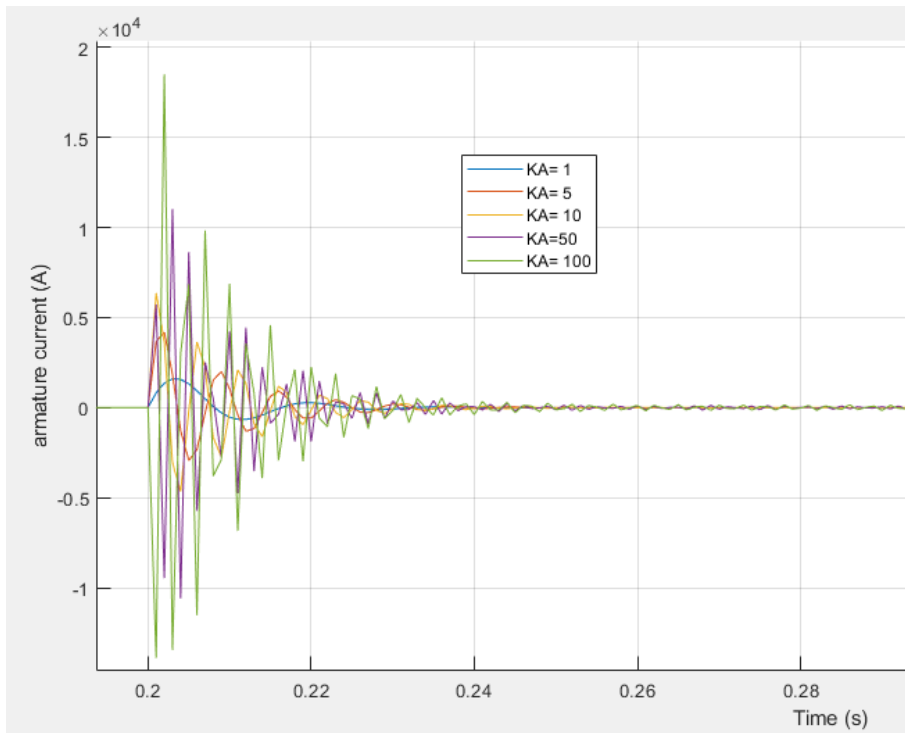


Fig. 18. Evolution of the armature current of the closed loop shunt excitation current machine with a PI corrector

Table 3 presents the initial values of the rotational speed of the shunt-wound DC motor in a closed-loop system with a PI controller for different values of the amplification gain K_A .

Table 3. Performance of the steady-state system of the direct current machine with closed-loop shunt excitation in control by supply voltage with a PI corrector, subjected to a variable load

Performances	$K_A = 1$	$K_A = 5$	$K_A = 10$	$K_A = 50$	$K_A = 100$
$\omega_{BF1C\ max}$ (rad/s)	215.74	253.53	253.91	282.62	262.48
$\omega_{BF1C\ moyen}$ (rad/s)	155.85	155.99	156.01	156.15	156.04
$\varepsilon_{BF1C\ moyen}$ (rad/s)	1.15	1.01	0.99	0.85	0.96
RMSE	1.17	0.99	0.98	1.08	1.10
Corrélation	0.8349	0.8395	0.8005	0.0359	0.4065
$\tau_{m\ BF1C}$ (ms)	4.5	2.5	1.5	1.5	1.5
$\tau_{r\ BF1C}$ (ms)	21.5	9.5	7.5	6.5	6.5
$I_{a\ BF1C\ max}$ (kA)	1.6	4.1	6.3	11.02	18.49
$I_{a\ BF1C\ moyen}$ (A)	6.39	6.32	6.31	14.36	-115.30
P(Hz)	-222.22	-400	-666.67	-666.67	-666.67
Stabilité	Stable	Stable	Stable	Stable	Stable

Overall, from these various results, we observe that increasing the amplification gain leads to an increase in the armature current. The system becomes more accurate as the steady-state error approaches zero with higher amplification gain. Additionally, the system responds faster with a higher amplification gain. Regardless of the amplification gain value, the closed-loop system with a PI controller remains stable.

7 CONCLUSION

Modelling the DC motor with excitation in Matlab/Simulink allowed us to perform its control by varying the armature voltage U_a , first in a closed-loop system without a controller and then in a closed-loop system with a PI controller. In this work, we observed that controlling the shunt-wound DC motor with two PI controllers (one for speed and one for current) provides good performance in terms of accuracy, rise time, stability, and especially speed, thanks to its speed coefficient λ . With this speed coefficient λ related to the amplification gain K_A , the control of the system with a single PI speed controller yielded an optimal result with $K_A=5$, achieving a correlation coefficient $R^2=0.8395$ and $RMSE = 0.99$. For the case of controlling the system with two PI controllers (one for speed and one for armature current), the best result was obtained with $K_A=5$, achieving a correlation coefficient $R^2=0.9990$ and $RMSE = 1.73$.

In the future, this work could be extended first to the study of the performance of both control methods, taking into account the transient response. It could also be expanded to examine the control of the DC motor by simultaneously adjusting both the excitation current I_e and the armature voltage U_a , and to investigate the performance of the system considering both the transient and steady-state conditions.

REFERENCES

- [1] T. Moulay «Machines à courant continu: Généralités et principe de fonctionnement des MCC,» Université de SAIDA, 2020.
- [2] K. Hartani, Y. Miloud et A. Miloudi, «Méthodologie Causal de modélisation et de commande: application aux machines électriques», Université Tahar Moulay de Saida, ALGERIE, 2009.
- [3] [3] G. Debbache et N. Kebaili, «Commande non linéaire de la machine à courant continu», Université Larbi Ben M'hidi Oum El Bouaghi, 2012-2013.
- [4] M. L. Sadeg et F. Yahiantene, «Etude et réalisation de la commande par retour d'état adaptative d'un moteur à courant continu», Université Djillali Liabes De Sidi Bel Abbes, 2015-2016.
- [5] Cossi Téléspore Nounangnonhou, Guy Clarence Semassou, Kossoun Alain Tossa, and Maryse Assogba, «Electrical and mechanical study of a medium-voltage overhead distribution line,» International Journal of Innovation and Applied Studies, vol. 42, no. 2, pp. 220–232, April 2024.
- [6] M. Kuczmann, «Review of DC Motor Modeling and Linear Control: Theory with Laboratory Tests». Electronics 2024.
- [7] «DC Electric Motors». Available online: https://www.transtecno.com/wordpress/wp-content/uploads/2015/06/H_EC-DCelectric-motors_210513_0521.pdf (accessed on 2 May 2024).
- [8] A. Baysse, «Contributions à l'identification paramétrique de modèles à temps continu: Extensions de la méthode à erreur de sortie, Développement d'une approche spécifique aux systèmes à boucles imbriquées», Toulouse: INP, 2010.
- [9] A. A. Awouda et M. M. Salih, Speed Control of DC Motor Using PI Controller, International Journal of Computer Science and Management Studies Vol. 15, Issue 06, 2015.
- [10] H. Huang, «PI Control Technology Principal Analysis and Simulation», Highlights in Science, Engineering and Technology, vol 71, 2023.